Threshold Based Vegetation Classification Using Sentinel-2 and Google Earth Engine in Siak-Riau

Elvira Nurrahma [1)*], Faiza Aulia Supriatna [2)], Inggit Lolita Sari [3)], Emilia Roza [4)], Harry Ramza [5)]
[1,2,4,5)] Department of Electrical Engineering, Faculty of Industrial Technology and Informatics
Universitas Muhammadiyah Prof. DR. Hamka
[3)] Research Center for Geoinformatics, The National Research and Innovation Agency of Indonesia (BRIN)
* Corresponding author : elviranurrahma27@gmail.com

Abstract
Land cover change driven by the expansion of oil palm plantations has become a critical environmental issue in Siak Regency, Riau Province, requiring periodic vegetation monitoring to support sustainable land management. This study presents a structured image processing workflow for multitemporal vegetation classification using Sentinel-2 Level-2A imagery from 2022 to 2024 implemented on Google Earth Engine. The workflow includes data collection, image pre-processing, vegetation index computation (NDVI, EVI, SAVI), threshold-based classification, spatial visualization using QGIS, and accuracy assessment. The workflow integrates cloud-based geospatial processing and threshold analysis for vegetation mapping. The results indicate that central and eastern areas of Siak Regency are dominated by moderate to dense vegetation, while western regions show gradual land conversion. In Koto Gasib District, oil palm plantation areas decreased from approximately 741,541 ha in 2022 to 709,815 ha in 2024, while non-oil palm and transitional land cover classes increased. The classification achieved an overall accuracy of 84.7% and a Kappa coefficient of 0.79, indicating reliable classification performance. The study shows the applicability of Google Earth Engine and Sentinel-2 imagery for multitemporal vegetation monitoring to support land use planning.

Keywords- Google Earth Engine, Land Cover Change, Multitemporal Classification, Oil Palm Monitoring, Sentinel-2, Vegetation Index

1. INTRODUCTION

Oil palm (Elaeis guineensis Jacq.) is a major plantation commodity contributing significantly to Indonesia's national economy. Riau Province possesses the largest oil palm plantation area in Indonesia, accounting for more than 21% of the national total, where expansion is often associated with decreasing vegetation density and declining environmental services [1]. The rapid expansion of oil palm plantations has driven land cover changes that affect ecosystem balance and environmental functions, highlighting the need for periodic spatial monitoring to support sustainable land management [2].

Remote sensing has become an effective approach for large-scale land cover monitoring. Sentinel-2 Level-2A imagery, equipped with the MultiSpectral Instrument (MSI), provides 10-meter spatial resolution and a 5-day revisit cycle, offering advantages for multitemporal vegetation analysis compared to conventional ground-based methods [3]. Multispectral vegetation indices, such as NDVI, EVI, and SAVI, have been widely used to quantitatively assess vegetation density and health conditions in tropical plantation environments [4-5]. Sentinel-2 was selected in this study due to its red-edge bands, 10-meter spatial resolution, and 5-day revisit cycle, which together offer superior capabilities for detecting subtle canopy density changes in oil palm plantations compared to Landsat (30 m, 16-day revisit) or MODIS (250–500 m) imagery [16-19].

The Google Earth Engine platform enables large-scale geospatial data processing through cloud-based computation, allowing complex analytical workflows to be executed without local data storage [6]. Previous studies have demonstrated high classification accuracy using GEE, with overall accuracy values exceeding 98% and strong Kappa agreement [7-8]. Various approaches have been applied, including threshold-based classification and machine learning methods such as Random Forest (RF) and Support Vector Machines (SVM) [9-12]. However, while machine learning methods often achieve higher

DOI : https://doi.org/10.21063/jtif.2026.V14.1.24-46

classification accuracy, they require labeled training data, substantial computational resources, and are less transparent in their decision logic. Studies specifically evaluating the trade-off between threshold-based and AI-driven approaches in terms of reproducibility, computational efficiency, and accuracy for multitemporal oil palm monitoring in tropical regions remain scarce [9-14].

Threshold-based classification remains widely used due to its computational efficiency, interpretability, and reproducibility [13-14]. However, three critical gaps persist in existing literature. First, previous studies have not systematically quantified whether threshold-based methods can match the accuracy of AI approaches (RF, SVM) specifically for oil palm monitoring when paired with multi-index inputs (NDVI,EVI, and SAVI) rather than a single index. Second, no standardized, reproducible computational pipeline has been published for multitemporal oil palm monitoring in Siak Regency, a region with the most extensive plantation area in Indonesia. Third, the transparency and scalability of existing workflows are rarely documented, making replication across time periods or regions difficult [13-15]. These limitations hinder operational vegetation monitoring and land management decision-making. This study addresses these gaps by developing and benchmarking a reproducible multi-index threshold-based classification framework on Google Earth Engine for multitemporal vegetation change analysis in Siak Regency over 2022–2024.

2. METHODS AND DATA

This research employs a structured six-stage computational image processing and classification framework to analyze vegetation dynamics in oil palm plantations in Siak Regency. The framework integrates Google Earth Engine for scalable cloud-based processing and QGIS for spatial visualization and cartographic production. Each stage produces outputs that serve as direct inputs to the subsequent stage, ensuring a traceable and reproducible analytical chain Figure 1.

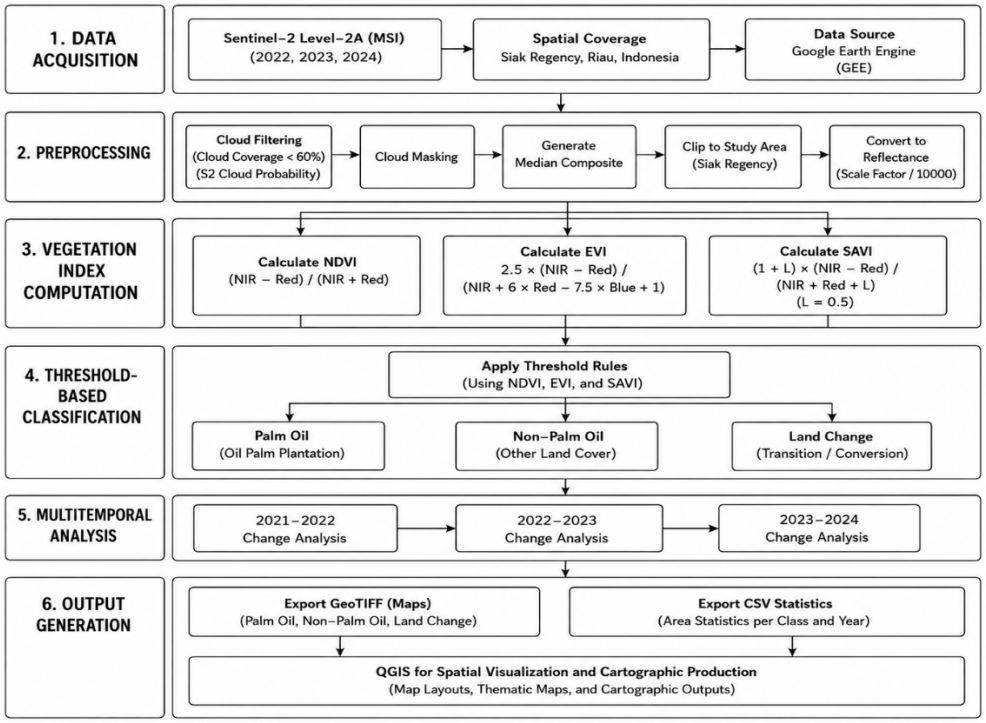

Figure 1. Research Framework

The complete framework is illustrated in Figure 1, which summarizes the sequential process from satellite data acquisition to change detection and final data export. Each stage is interconnected, where the output

DOI : https://doi.org/10.21063/jtif.2026.V14.1.24-46

of one stage serves as the input for the subsequent stage, ensuring a consistent, traceable, and reproducible analytical framework.

2.1 Data Collection

This research began by defining the study area boundaries using administrative shapefiles of Siak Regency, Riau Province. The vector data was uploaded to Google Earth Engine as an asset and used as the primary spatial boundary throughout the analysis process. With this approach, the entire image data collection process was strictly limited to the study area, thereby increasing computational efficiency and maintaining spatial consistency across time [6-9].

The primary data used was Sentinel-2 Level-2A imagery (COPERNICUS/S2_SR_HARMONIZED), which underwent atmospheric correction using the Sen2Cor algorithm. Sentinel-2 was chosen because of its advantages of high spatial resolution (10–20 m), broad spectral coverage (13 bands), and relatively fast revisit time (±5 days). These characteristics make it highly suitable for monitoring rapidly changing tropical vegetation dynamics, such as in oil palm plantations [16-19][27]. Compared with previous studies that generally used Landsat imagery (30 m) or data with lower temporal resolution, Sentinel-2 provides significant improvements in the ability to detect small-scale vegetation changes and variations in canopy density. The presence of red-edge bands is also an important advantage because it is more sensitive to chlorophyll content and vegetation stress conditions, which were not available with previous-generation sensors [16-19].

To maintain temporal consistency, data was filtered by annual period (January–December) for 2022, 2023, and 2024. Furthermore, an initial filtering of cloud cover ≤ 20% was performed using the CLOUDY_PIXEL_PERCENTAGE metadata to reduce images with high cloud cover before masking at the pixel level [18]. During the analysis process, several key bands were selected with high sensitivity to vegetation and land surface conditions: B2 (Blue, 490 nm), B3 (Green, 560 nm), B4 (Red, 665 nm), B8 (Near Infrared, 842 nm), B11 (SWIR-1, 1610 nm), and B12 (SWIR-2, 2190 nm). The Red and NIR bands are used as the primary basis for vegetation analysis, such as NDVI [5][11][14], while the Blue band is used for atmospheric correction and the calculation of vegetation-based indices, such as EVI [21]. Meanwhile, the SWIR band plays a role in detecting vegetation moisture and soil characteristics, thus assisting in the separation of land cover classes [19][23].

All key bands have a spatial resolution of 10 meters for the high-resolution bands (B2, B3, B4, and B8), allowing for detailed spatial analysis at the landscape level. This multi-band combination allows for the extraction of more comprehensive vegetation information, both in terms of density, health, and surface biophysical conditions [19][14]. Details of the spectral characteristics of the Sentinel-2 Multispectral Instrument (MSI), including the wavelength and spatial resolution of each band, are presented in Table 1.

Table 1. Sentinel-2 Spectral Bands

No	Band	Band Name	Wavelength (nm)	Resolution	Description
1.	B1	Coastal Aerosol	443	60 m	Aerosol detection and atmospheric correction.
2.	B2	Blue	490	10 m	Natural color, bathymetry, EVI, and cloud masking.
3.	B3	Green	560	10 m	Natural color and vegetation health assessment.
4.	B4	Red	665	10 m	NDVI, EVI, SAVI, and chlorophyll absorption sensitivity.
5.	B5	Red Edge 1	705	20 m	Initial vegetation structure analysis.

DOI : https://doi.org/10.21063/jtif.2026.V14.1.24-46

No	Band	Band Name	Wavelength (nm)	Resolution	Description
6.	B6	Red Edge 2	740	20 m	Vegetation change detection.
7.	B7	Red Edge 3	783	20 m	Biophysical vegetation analysis.
8.	B8	Near Infrared (NIR)	842	10 m	NDVI, EVI, SAVI, and vegetation biomass monitoring.
9.	B8A	Narrow NIR	865	20 m	Specific vegetation analysis.
10.	B9	Water Vapour	945	60 m	Atmospheric water vapor correction.
11.	B10	SWIR – Cirrus	1375	60 m	Detection of cirrus clouds.
12.	B11	SWIR 1	1610	20 m	Cloud masking, soil moisture, and vegetation water content.
13.	B12	SWIR 2	2190	20 m	Cloud masking, dry soil identification, and fire detection.

2.2 Image Pre- Processing

In the pre-processing stage, cloud masking was performed using the Scene Classification Layer (SCL) from the Sentinel-2 Level-2A product. SCL provides pixel classification based on surface and atmospheric conditions, including vegetation, water, bare ground, clouds, and cloud shadows. In this study, pixels with classes 3 (cloud shadow), 8 (medium probability cloud), 9 (high probability cloud), and 10 (cirrus cloud) were removed from the analysis due to their potential to distort surface reflectance values [17]. This SCL-based approach is more stable than simple masking because it has undergone Sentinel-2 Level-2A's built-in atmospheric classification process, thus improving the accuracy of spectral data for vegetation analysis [17-18].

After masking, annual composites were formed using the median reducer method on all filtered images for each January–December period (2022–2024). The median method was chosen because it is more robust against outliers such as residual clouds, shadows, and extreme temporal phenomena (e.g., floods or fires). This approach produces a stable spectral representation that is more representative of the average land surface conditions over a single observation year [18][19]. In its implementation, this process is performed using the ee.Reducer.median() function in Google Earth Engine, which is commonly used in large-scale time series analysis due to its ability to reduce noise without losing important information from multi-temporal data [6][18].

The final result of this stage is a cloud-free annual composite image for 2022, 2023, and 2024. All images are then cropped according to the study area boundaries and reprojected into the UTM coordinate system (EPSG:32748/32749) with a spatial resolution of 10 meters. This data is then used as the primary input for calculating the vegetation index in the next stage [19][21].

2.3 Vegetation Index Computation

Three vegetation indices are derived from annual median composite images to characterize vegetation conditions from different spectral perspectives. Each index captures specific biophysical properties of vegetation, providing complementary information for land cover analysis [19]. This multi-index

DOI : https://doi.org/10.21063/jtif.2026.V14.1.24-46

approach is necessary because a single index is often insufficient to represent complex vegetation conditions in oil palm plantation environments.

The first index is the Normalized Difference Vegetation Index (NDVI), which measures the spectral contrast between red and near-infrared (NIR) reflectance. This contrast reflects chlorophyll absorption in the red band and strong reflectance from leaf cellular structure in the NIR band. NDVI is widely used in vegetation mapping due to its simplicity and effectiveness, including applications in oil palm monitoring in tropical regions [4][5][20].

$$NDVI = \frac{NIR - RED}{NIR + RED} \quad (1)$$

NDVI values range from -1 to +1, where higher values indicate denser vegetation cover. The classification scheme is provided in Table 2.

Table 2. NDVI Index Classification [19]

Division area	NDVI value
Non-Vegetation	-1 ≤ NDVI < 0,2
Sparse Vegetation	0,2 < NDVI < 0,4
Moderate Vegetation	0,4 < NDVI < 0,6
Dense Vegetation	0,6 NDVI ≤ 1

Although the Normalized Difference Vegetation Index (NDVI) is used in vegetation analysis, it has limitations, particularly in areas with high biomass, where index values tend to saturate, making it less sensitive in distinguishing high variations in vegetation density. Therefore, this study used an additional index, the Enhanced Vegetation Index (EVI), to complement the analysis.

The EVI was developed to reduce the influence of atmospheric disturbances and background canopy and soil effects, thus providing a more accurate estimate of vegetation condition, particularly in areas with dense vegetation cover, such as oil palm plantations [21]. Unlike the NDVI, the EVI integrates the blue band in its calculation to assist with atmospheric correction and uses an empirical gain factor to increase sensitivity to vegetation signals. Generally, EVI values range from -1 to +1, with healthy vegetation typically having values between 0.20 and 0.80. Higher values indicate denser and more productive vegetation, while lower values indicate sparse or non-vegetated vegetation. Mathematically, EVI is formulated as:

$$EVI = 2.5 \frac{(NIR - RED)}{(NIR + 6 \times RED - 7.5 \times BLUE + 1)} \quad (2)$$

The third index used is the Soil-Adjusted Vegetation Index (SAVI), which is designed to reduce the influence of soil reflectance, especially in areas with sparse vegetation cover. This is particularly relevant in the context of oil palm plantations, where some areas between plant canopies often still reveal bare soil. SAVI introduces a soil correction factor (L), which in this study was set at 0.5 as the default value for moderate vegetation conditions [22-23]. The SAVI equation is expressed as:

$$SAVI = \frac{(NIR - RED)}{(NIR + RED + L)}(1 + L) \quad (3)$$

SAVI values range from -1 to +1, with high positive values indicating healthy vegetation density and greenness, while negative values represent areas with minimal vegetation or areas dominated by ground

DOI : https://doi.org/10.21063/jtif.2026.V14.1.24-46

light reflection. This index is designed as a qualitative descriptor to minimize the influence of background soil, especially in areas with sparse vegetation cover, with the full classification range shown in Table 3.

Table 3. SAVI Classification [21]

Density Range	SAVI Value Classification
Non-Vegetation	-1 – -0.29
Low	-0.29 – 0.26
Moderate	0.26 – 0.66
High	0.66 – 0.99
Very High	0.99 – 1.38

The combination of NDVI, EVI, and SAVI provides a more robust representation of vegetation conditions by capturing variations in greenness, biomass density, and soil background influence. The resulting output is a three-band raster consisting of NDVI, EVI, and SAVI layers. This dataset is exported from Google Earth Engine to Google Drive in GeoTIFF format at 10-meter spatial resolution and projected to the appropriate UTM coordinate system (EPSG:32748 or EPSG:32749). These layers are subsequently used as input for land cover classification.

2.4 Threshold-Based Classification

Threshold-based classification assigns land cover categories to each pixel based on whether its vegetation index value falls within a predefined numerical range. This method is computationally efficient, fully transparent in its decision logic, and reproducible across datasets without requiring training samples, making it highly suitable for operational vegetation monitoring applications [13][14]. The classification thresholds applied in this study are informed by the seminal vegetation index literature [24][25][26] and adapted for tropical oil palm environments.

For NDVI, pixels are classified into five classes according to the scheme in Table 2, with the critical threshold of NDVI ≥ 0.3 separating non-vegetated from vegetated surfaces. classification for EVI based on initial values before adjustments are made based on data, and SAVI is classified according to Table 3. The binary oil palm vs. non-oil palm classification used for the Koto Gasib analysis applies NDVI ≥ 0.5 as the primary discriminant for oil palm canopy identification, consistent with spectral profiles documented for mature oil palms in tropical conditions [27].

The GEE JavaScript implementation encodes the classification as a series of conditional image operations (ee.Image.where()), producing a discrete classified raster as the output. This algorithmic pipeline can be reproduced in full from the documented code and constitutes the primary computer science contribution of this research: a structured, replicable image classification workflow implemented in a cloud computing environment.

2.5 Spatial Visualization in QGIS

The classified GeoTIFF rasters exported from Google Earth Engine were then imported into QGIS software for map production (cartography). At this stage, each raster layer was first verified for its coordinate reference system (CRS) to ensure that all data was in a consistent projection, preventing spatial shifts between layers.

Following the CRS verification process, the symbology of each raster was adjusted using a color ramp that visually represents vegetation classes. The color scheme used was red for non-vegetation, orange

DOI : https://doi.org/10.21063/jtif.2026.V14.1.24-46

for very low vegetation, yellow for low vegetation, light green for medium vegetation, and dark green for dense vegetation. This color scheme aimed to enhance visual interpretation of the spatial distribution of vegetation conditions in the study area.

The final map was then compiled using the Print Layout module in QGIS, which allows for the systematic integration of various cartographic elements. Elements included in the map composition include a legend to explain vegetation classes, a scale bar to indicate spatial distance, a north arrow for map orientation, and an inset map showing the location of Siak Regency within the context of Riau Province. The addition of these elements aims to improve the readability, completeness of information, and scientific standards of the resulting map. All final maps are exported in PNG and PDF formats at a minimum resolution of 300 dpi to ensure high visual quality and meet scientific and academic publication standards [28].

2.6 Accuracy Assessment

Accuracy assessment was performed through a stratified random sampling strategy to generate ground truth reference data for the classified maps. A minimum of 50 reference points per vegetation class were collected, distributed proportionally to class area using stratified random placement. Reference labels were assigned through visual interpretation of high-resolution Google Earth imagery and cross-checking against available field knowledge, a procedure consistent with established remote sensing accuracy assessment protocols [29].

Based on the confusion matrix, several key accuracy metrics were derived, namely Overall Accuracy (OA), Producer's Accuracy (PA), User's Accuracy (UA), and Kappa Coefficient (κ). Overall Accuracy (OA) describes the overall percentage of data correctly classified across all tested samples, thus providing a general overview of the classification success rate. Mathematically, OA is calculated as the ratio of the number of correct samples on the main diagonal of the confusion matrix to the total number of samples.

$$OA = \frac{\sum_{i=1}^{k} X_{ii}}{N} \quad (4)$$

Description:
X_{ii} = Diagonal value (correct classification in class i)
N = Total of all samples
k = Number of classes

Producer's Accuracy (PA) is used to measure accuracy from a reference data perspective and is related to omission error, which is the number of actual objects in a class that are correctly detected by the classification model where this value indicates the proportion of reference samples in a particular class that were successfully classified correctly. Mathematically, PA is formulated as:

$$PA_i = \frac{X_{ii}}{\sum_{j=1}^{k} X_{ij}} \quad (5)$$

Description:
X_{ii} = Number of true samples in class i
$\sum X_{ij}$ = Total references in class i

In contrast, User's Accuracy (UA) indicates accuracy from a map results perspective and is related to commission error, which is the degree to which we can be confident that the mapped classes truly correspond to actual conditions in the field which describes the proportion of truth of a class in the classification results against all pixels mapped to that class. Mathematically, UA is expressed as:

DOI : https://doi.org/10.21063/jtif.2026.V14.1.24-46

$$UA_i = \frac{X_{ii}}{\sum_{j=1}^{k} X_{ji}} \quad (6)$$

Description:
X_{ii} = Number of true samples in class i
$\sum X_{ji}$ = Total classification results in class i

In addition, the Kappa Coefficient ($\varkappa$) is also used to measure the level of agreement between the classification results and the reference data, taking into account the possibility of random agreement. Thus, the Kappa value provides a more robust measure of accuracy than using only Overall Accuracy, which takes into account both actual agreement and random expected agreement. Mathematically, the Kappa Coefficient is formulated as:

$$k = \frac{N \sum X_{ii} - \sum (X_{i+} X_{+i})}{N^2 - \sum (X_{i+} X_{+i})} \quad (7)$$

Description:
N = Total sample
X_{ii} = Main diagonal of the confusion matrix
X_{i+} = Total of row i
X_{+i} = Total of column i

Acceptance thresholds follow the criteria of Landis and Koch [30]: OA ≥ 80% and $\varkappa \geq 0.60$ are required for the classification to be considered satisfactory. If thresholds are not met, the classification parameters (index thresholds, class boundaries) are revised iteratively.

3. RESULTS AND DISCUSSION

The Siak Regency administrative boundaries in shapefile (SHP) format were successfully uploaded to Google Earth Engine as an asset and verified with official boundary data issued by the Quantum Geographic Information System to ensure spatial suitability and geometric accuracy of the study area. The study area covers a total area of approximately 841,798 hectares and encompasses 14 sub-districts within Siak Regency. This information demonstrates the spatial scope of the analysis used in the study.

The annual Sentinel-2 Level-2A image collection, filtered for the periods of 2022, 2023, and 2024, and clipped to the ROI boundaries, yielded 387 scenes (2022), 412 scenes (2023), and 398 scenes (2024), respectively, before cloud pre-filtering. This demonstrates the availability of sufficiently dense imagery data for time series analysis.

After applying scene-level filtering based on a cloud cover threshold of ≤ 20%, the number of images used in the analysis was reduced because only scenes with good spatial quality were retained. This process ensured that the data used for the composite had minimal cloud interference, making it more reliable for further analysis. Figure 2 shows the administrative boundaries of the Siak Regency SHP that have been integrated and displayed in the Google Earth Engine environment, which serves as the spatial basis for the entire analysis process.The Siak Regency shapefile (SHP) data was integrated into Google Earth Engine to delimit the study area.

DOI : https://doi.org/10.21063/jtif.2026.V14.1.24-46

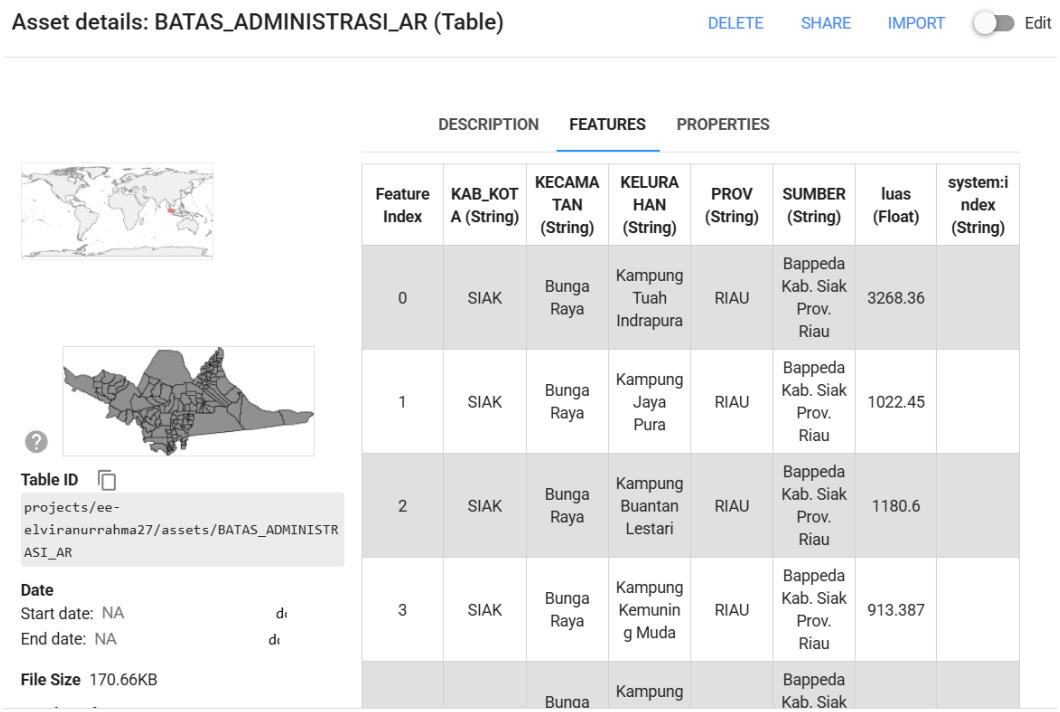

Figure 2. SHP File Administrative Boundaries AR Siak Regency

The pre-processing process begins with the application of cloud masking using the Scene Classification Layer (SCL) bands available in the Sentinel-2 Level-2A data. At this stage, pixels identified as atmospheric disturbances are eliminated from the dataset, specifically pixels belonging to SCL classes 3 (cloud shadows), 8 (medium-probability clouds), 9 (high-probability clouds), and 10 (thin cirrus clouds). This process is performed on each image in the annual collection, ensuring that only pixels with clear optical conditions are retained for further analysis.

The results of this process indicate that approximately 12–18% of pixels in each annual image stack were successfully removed, with the number varying depending on the cloud climatology of each year. In 2022, the highest frequency of cloud cover was recorded, particularly in the western districts of Tualang and Kandis. This condition resulted in small amounts of cloud-shadow artifacts remaining in certain locations, despite the SCL-based masking process.

To address these remaining disturbances, the subsequent stage in the framework involves temporal compositing using the median compositing method, as illustrated in Figure 3. At this stage, all masked images are combined into a single annual representative image by calculating the median value for each pixel. This approach is effective in reducing outliers, including those caused by residual cloud shadows and seasonal vegetation variations associated with flooding or drought conditions.

DOI : https://doi.org/10.21063/jtif.2026.V14.1.24-46

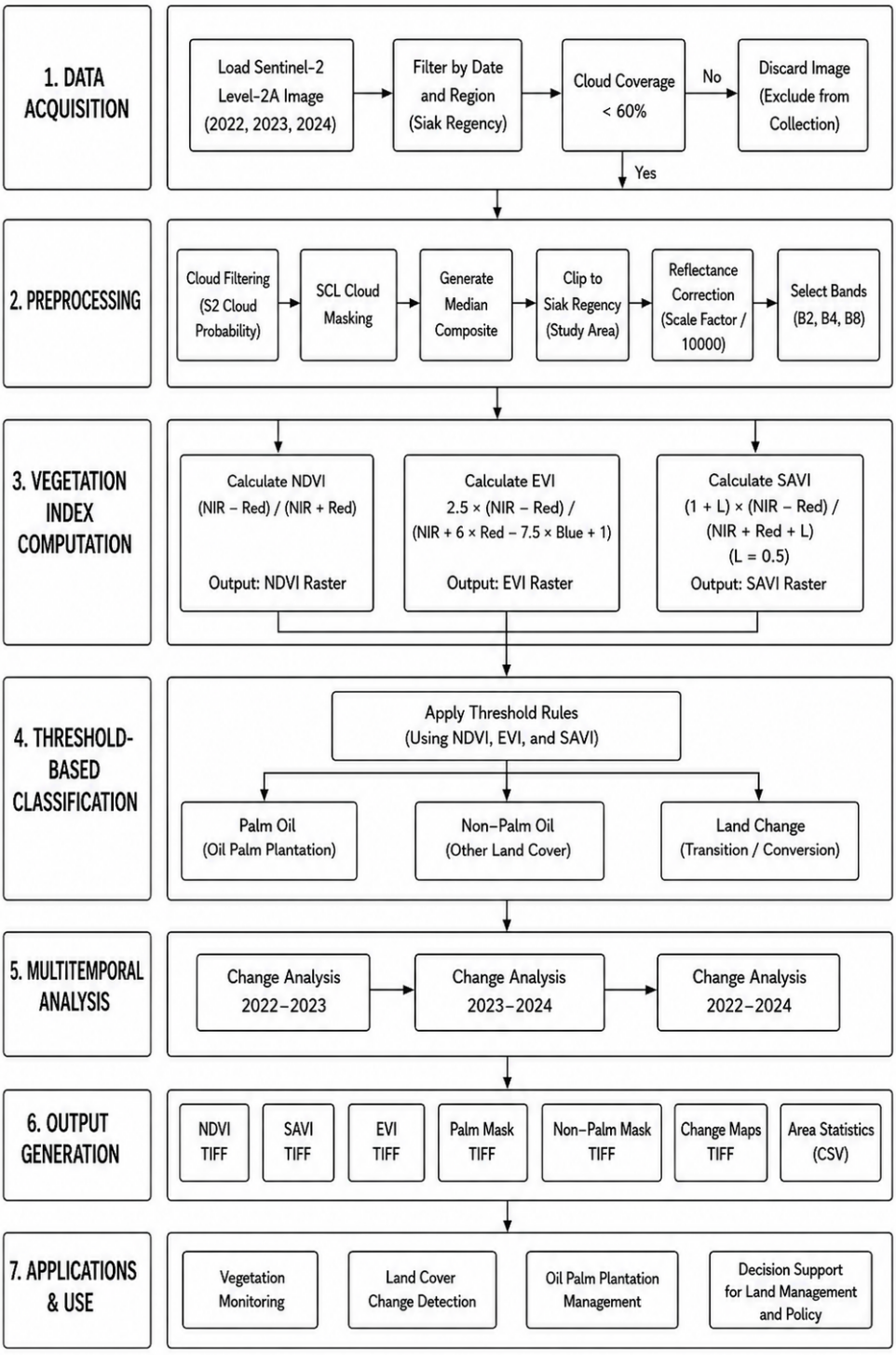

Figure 3. Research Framework for Multitemporal Vegetation Monitoring in Siak Regency (2022-2024) Using Sentinel-2 on Google Earth Engine

As a result, a stable, radiometrically consistent, and relatively cloud-free median annual composite image was obtained for each research year (2022, 2023, and 2024). This radiometric consistency is crucial because it ensures that reflectance values between pixels can be validly compared in subsequent analyses, particularly in calculating vegetation indices. Next, the processed composite images are exported in GeoTIFF format with a spatial resolution of 10 meters to Google Drive. This data is then used to calculate vegetation indices (NDVI, EVI, and SAVI) according to the research framework.

DOI : https://doi.org/10.21063/jtif.2026.V14.1.24-46

The final results of this stage can be seen in Figure 4, which shows the results of processing and classification based on composite imagery in the Google Earth Engine environment. The figure shows the spatial distribution of the classification results after going through the cloud masking and median composite stages, resulting in a cleaner and more representative map for further analysis.

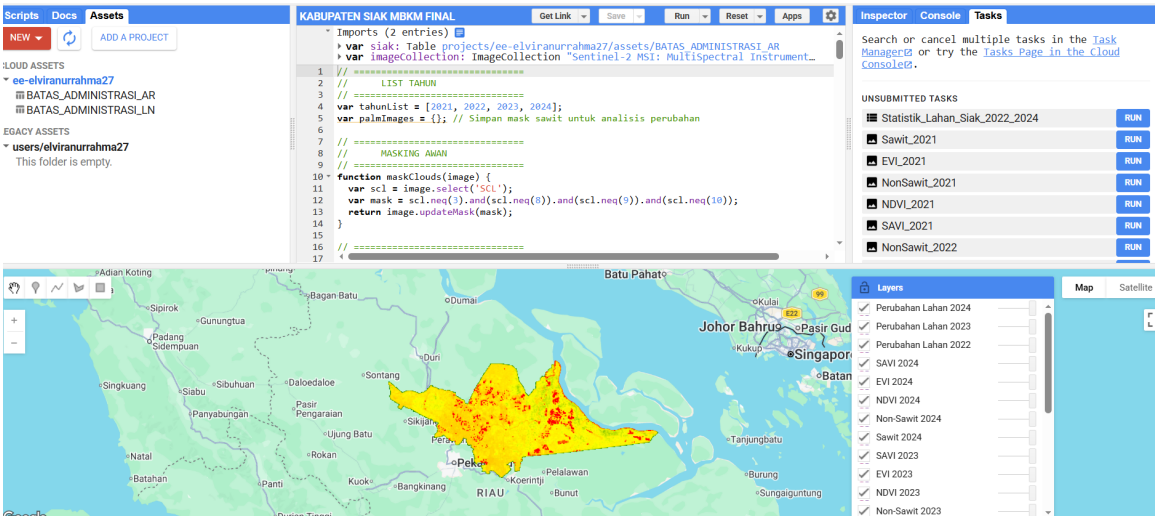

Figure 4. Classification Results in GEE Siak Regency

Vegetation indices were calculated at the pixel level (per pixel) for all annual composite images generated in the previous step. This means that each pixel in the image was analyzed individually to obtain a vegetation index value based on its spectral reflectance value. The resulting NDVI, EVI, and SAVI rasters were then saved and exported in multiband GeoTIFF format, so that all three indices were contained in the same raster file and could be analyzed simultaneously in QGIS. Summary statistics for each resulting vegetation index, such as minimum and maximum values, and value distribution, are presented in the subsequent classification section as a basis for determining threshold classification.

The resulting vegetation index raster shows a strong spectral contrast between densely vegetated areas in the central and eastern parts of Siak Regency, such as Dayun, Lubuk Dalam, and Koto Gasib, and western areas such as Tualang, Minas, and Kandis, which are dominated by mixed industrial and residential land uses. This pattern is consistent with previously known land use conditions in the region.

All vegetation indices (NDVI, EVI, and SAVI) were calculated within Google Earth Engine using standard band arithmetic operations, such as comparisons between the near-infrared (NIR), Red, and Blue bands. The results were then validated by comparing the resulting pixel value distributions with published spectral profiles for tropical vegetation and oil palm plantations. This validation process aimed to ensure that the obtained index values were within a reasonable range and consistent with the characteristics of the actual vegetation.

3.1 Processing Results in QGIS

The process of exporting raster data in Tagged Image File Format (GeoTIFF) from a cloud computing platform is followed by advanced spatial visualization and analysis steps within QGIS software, as shown in Figure 5.

DOI : https://doi.org/10.21063/jtif.2026.V14.1.24-46

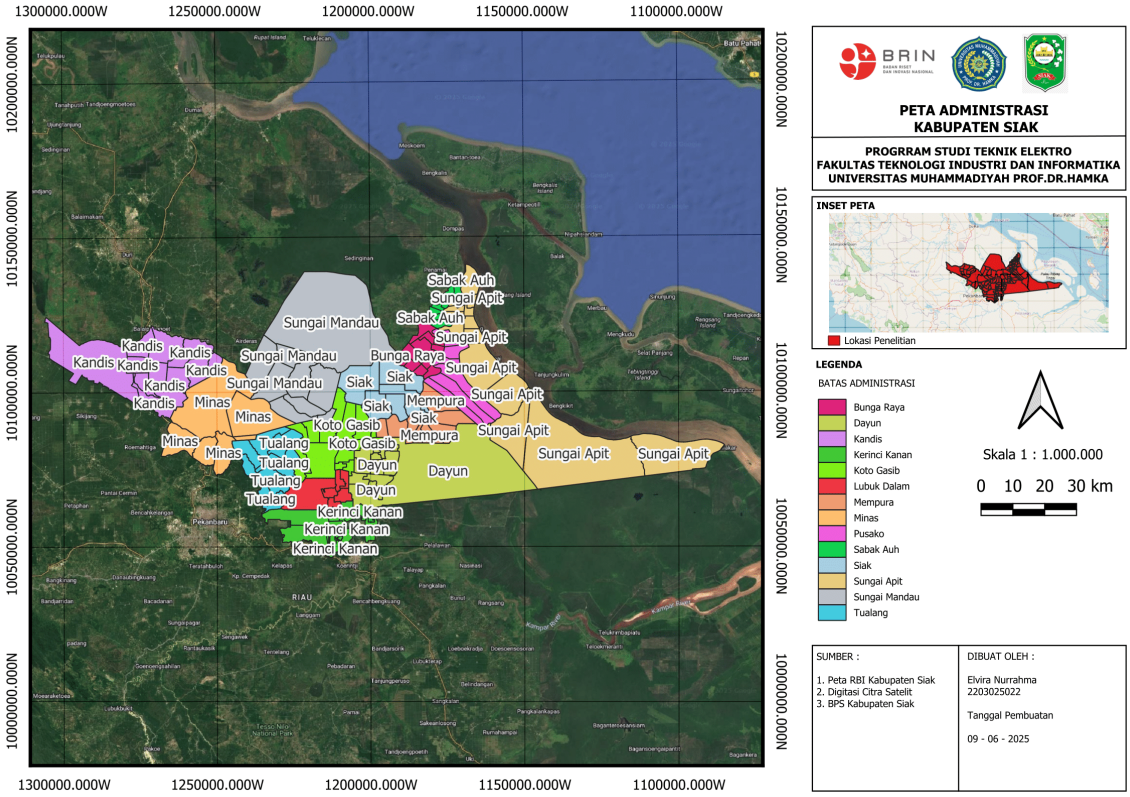

Figure 5. Administrative Boundaries of Siak Regency

An administrative map of Siak Regency, Riau Province, is presented in a 1:1,000,000 scale geographic coordinate system with distinct color divisions for easy visual identification across 14 sub-districts, spanning from Bunga Raya to Tualang. Geographically, this region is characterized by the dominant flow of the Siak River in the central part and is complemented by an inset map to show the relative position of the research location within the overall Riau Province.

3.2 NDVI Classification

Spatial analysis for the 2022–2024 period identified five classes of vegetation density, ranging from non-vegetation to dense vegetation, with a consistent dominance of moderate to dense vegetation in the central and eastern parts of Siak Regency Figure 6. This area includes the sub-districts of Dayun, Lubuk Dalam, Koto Gasib, and part of Sungai Apit, which are functionally oil palm plantations, production forests, and areas with preserved natural vegetation.

Meanwhile, very low to non-vegetation vegetation is generally distributed in the western and southwestern regions, such as Tualang, Kandis, and parts of Minas Districts, which are dominated by dense settlements, industrial activities, and land clearing. Between 2022 and 2023, a significant increase was detected from low to medium or dense vegetation, influenced by the growth of new oil palm plantations, the recovery of secondary vegetation, or rainfall patterns. However, in 2024, there was a further decline in vegetation quality in the western region due to new land clearing activities, land conversion, and seasonal factors such as a long drought during the satellite data acquisition period.

DOI : https://doi.org/10.21063/jtif.2026.V14.1.24-46

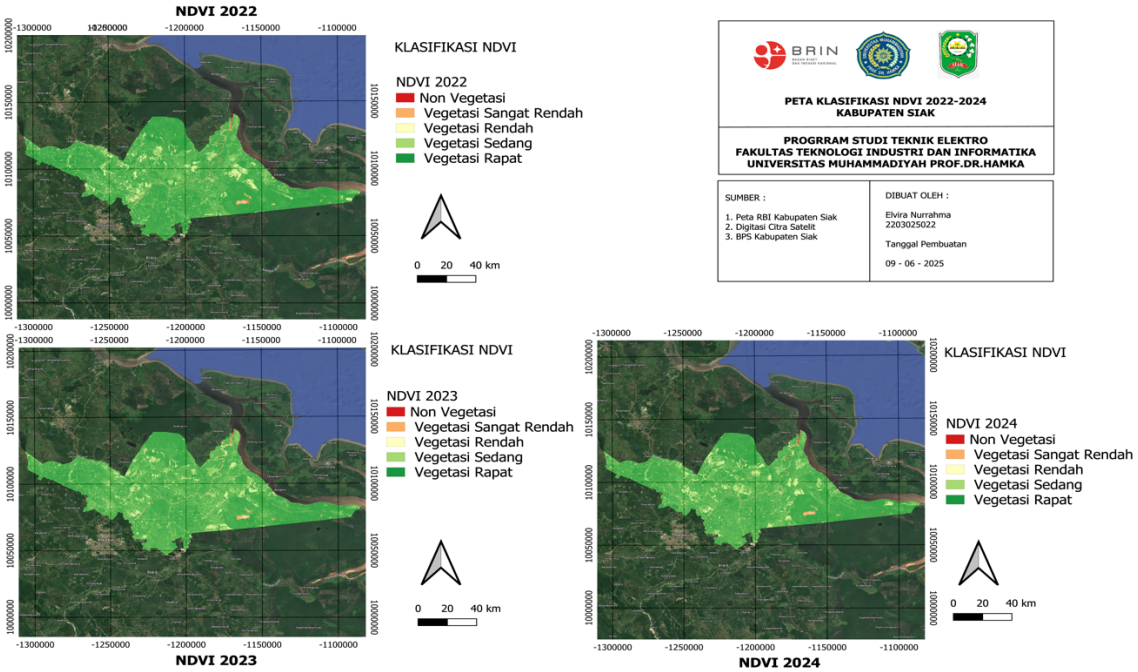

Figure 6. NDVI Classification Map of Siak Regency 2022–2024

As shown in Table 4, the NDVI classification results indicate fluctuations in vegetation conditions in Siak Regency throughout the 2022–2024 period. In 2022, the highest NDVI value reached >0.916 (dense vegetation), which dominated the central and eastern regions, while the lowest value was -0.422 (non-vegetation), concentrated in industrial and residential areas such as Tualang and Minas. In 2023, there was an increase in the upper limit of the NDVI value to >0.926, indicating oil palm growth or vegetation regeneration, while the minimum value decreased to -0.585 due to the expansion of bare land or waterlogging areas. Entering 2024, the maximum value slightly decreased to >0.912, accompanied by shifts in the lower limits of the low and moderate vegetation classes, indicating dynamic changes and localized declines in vegetation density in certain areas.

Table 4. The results of the NDVI classification of Siak Regency for 2022-2024

NDVI Classification	2022	2023	2024
Non Vegetation	-0,422 – -0,087	-0,585 – -0,207	-0,553 – -0,186
Very Low Vegetation	-0,087 – 0,246	-0,207 – 0,170	-0,186 – 0,179
Low Vegetation	0,246 – 0,581	0,170 – 0,548	0,179 – 0,546
Moderate Vegetation	0,581 – 0,916	0,548 – 0,926	0,546 – 0,912
Dense Vegetation	>0,916	>0,926	>0,912

Table 4 summarizes the NDVI classification thresholds applied for vegetation density categorization in Siak Regency during the 2022–2024 observation period. The overall research framework and classification process used to generate the NDVI-based vegetation classes are illustrated in Figure 7. The framework summarizes the sequential stages of data acquisition, preprocessing, NDVI computation, threshold-based classification, and interpretation of vegetation density levels. Each stage is systematically connected, where the output produced from one process serves as the input for the subsequent process, thereby ensuring consistency throughout the vegetation classification analysis.

DOI : https://doi.org/10.21063/jtif.2026.V14.1.24-46

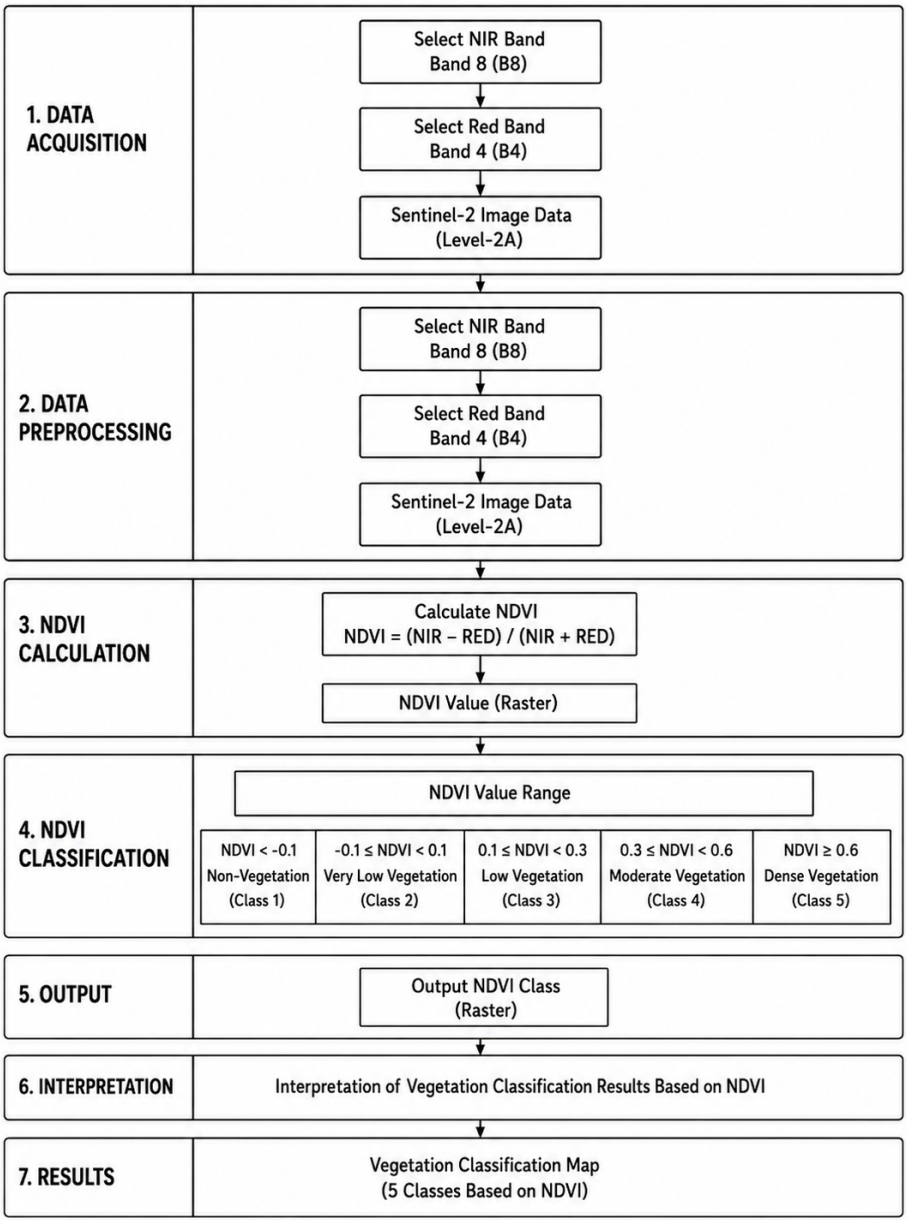

Figure 7. NDVI Classification Framework for Siak Regency 2022-2024

3.3 EVI Classification

The Enhanced Vegetation Index (EVI) classification in this study is divided into five levels of vegetation density, namely non-vegetation to dense vegetation, which is visualized through a color gradation from red to dark green to facilitate spatial analysis. Based on Figure 8, the central and eastern regions of Siak Regency, such as Dayun, Lubuk Dalam, and Koto Gasib Districts, are dominated by moderate to dense vegetation classes indicating high and stable vegetation cover for three years, while the Tualang, Kandis, and parts of Minas areas are dominated by very low to non-vegetation classes due to industrial activities, development, or open land.

From 2022 to 2023, vegetation density increased in several areas due to plant growth or land restoration, but in 2024 there was a decrease in the western and southeastern parts triggered by land clearing or dry weather factors at the time of image capture. Overall, this pattern indicates that although vegetation in Siak Regency is relatively stable, annual fluctuations still occur influenced by the interaction between environmental factors and human activities.

DOI : https://doi.org/10.21063/jtif.2026.V14.1.24-46

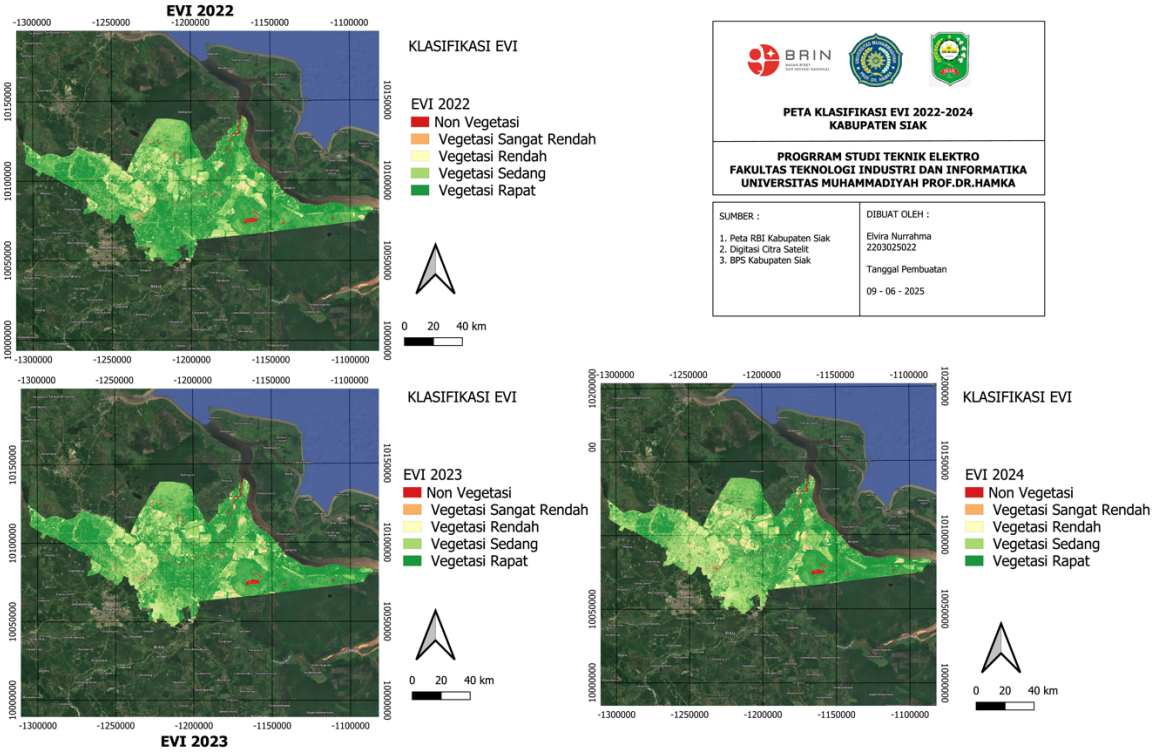

Figure 8. EVI Classification Map of Siak Regency 2022–2024

Based on table 5 below, the range of EVI classification values in 2022 ranges from -0.021 to more than 0.605, with the non-vegetation category in the range of -0.021 to -0.135, very low vegetation -0.135 to 0.292, low vegetation 0.292–0.448, medium vegetation 0.448–0.605, and dense vegetation above 0.605. In 2023, the classification pattern shows a slight shift in the boundary values where non-vegetation is in the range of -0.015 to 0.139, very low vegetation 0.139 to 0.295, low vegetation 0.295–0.450, medium vegetation 0.450–0.605, and dense vegetation remains above 0.605. Meanwhile, in 2024, there will be another adjustment to the limit values due to fluctuations in weather factors and planting seasons, with a non-vegetation range of -0.016 to 0.143, very low vegetation 0.143–0.302, low vegetation 0.302–0.462, moderate vegetation 0.462–0.622, and values above 0.622 are categorized as dense vegetation.

Table 5. The results of the EVI classification of Siak Regency for 2022-2024

EVI Classification	2022	2023	2024
Non Vegetation	-0,021 – -0,135	-0,015 – 0,139	-0,016 – 0,143
Very Low Vegetation	-0,135 – 0,292	0,139 – 0,295	0,143 – 0,302
Low Vegetation	0,292 – 0,448	0,295 – 0,450	0,302 – 0,462
Moderate Vegetation	0,448 – 0,605	0,450 – 0,605	0,462 – 0,622
Dense Vegetation	> 0,605	> 0,605	> 0,622

DOI : https://doi.org/10.21063/jtif.2026.V14.1.24-46

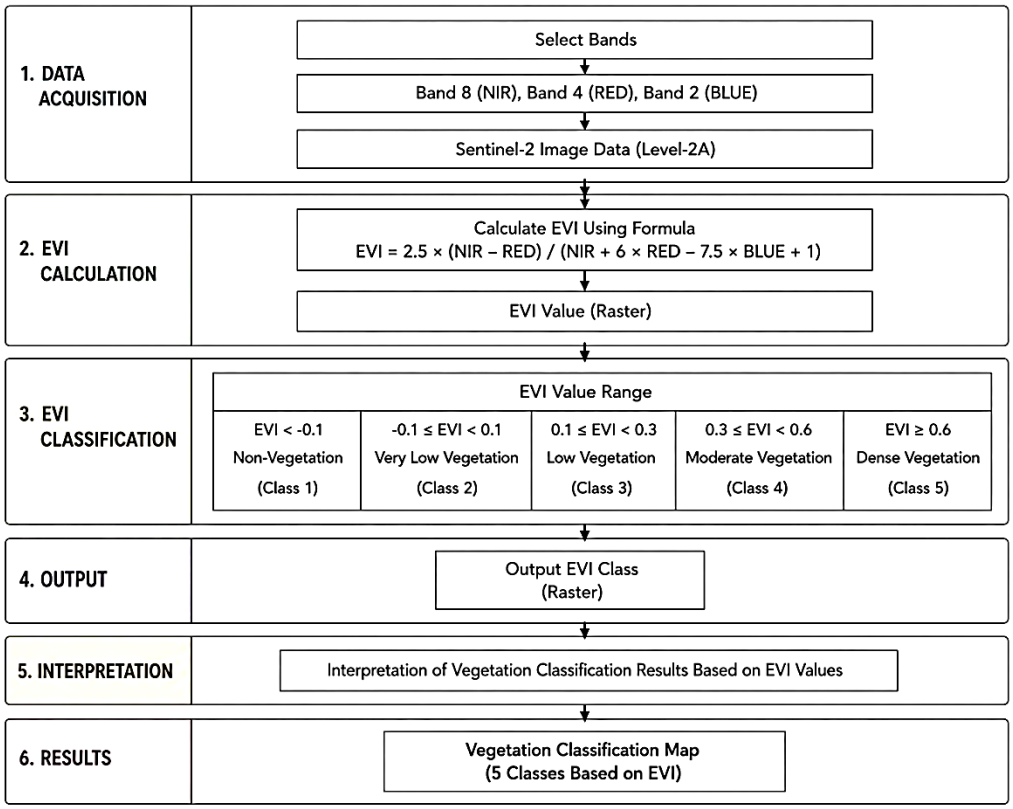

Figure 9. EVI Classification framework for Siak Regency 2022-2024

Figure 9 presents the research framework adopted for EVI based vegetation analysis in Siak Regency. The framework outlines a structured sequence of processes beginning with Sentinel-2 data preparation, followed by EVI calculation and vegetation classification using predefined threshold values, and ending with the production of thematic output maps. The integration of these stages enables a systematic and reproducible approach for identifying vegetation density patterns across the research area.

3.4 SAVI Classification

Spatial analysis using the Soil Adjusted Vegetation Index (SAVI) classification for the 2022 to 2024 period shows a consistent temporal distribution of vegetation in Siak Regency. In 2022, the central and eastern regions, such as Dayun, Koto Gasib, and Lubuk Dalam Districts, were dominated by moderate to dense vegetation. In 2023, moderate vegetation expanded in several low-density areas, indicating canopy development. Meanwhile, dense vegetation remained stable in the central part of the region, while low-density vegetation was concentrated around residential areas and open areas, as shown in Figure 10.

DOI : https://doi.org/10.21063/jtif.2026.V14.1.24-46

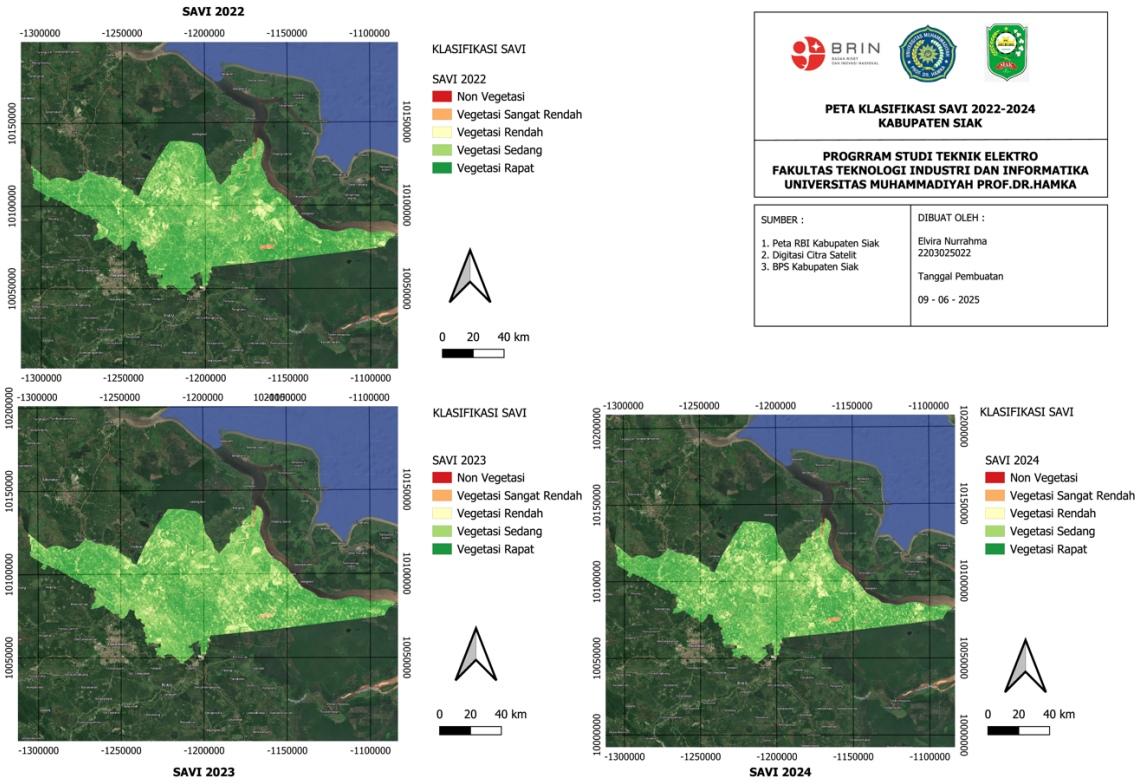

Figure 10. SAVI Classification Map of Siak Regency 2022–2024

Entering 2024, dense vegetation patterns persisted across most of the central and eastern regions, although there was a decline to low to very low levels in the western and southwestern regions, such as Tualang and Kandis Districts, due to potential land clearing or seasonal factors. Non-vegetated areas and very low vegetation were consistently concentrated in densely populated and industrial areas, including Tualang, Minas, and Kandis, which are dominated by open land and buildings. This phenomenon also demonstrates the superiority of the SAVI index in accurately representing vegetation conditions in areas with mixed land cover that have high soil reflectance.

Table 6. The results of the SAVI classification of Siak Regency for 2022-2024

SAVI Classification	2022	2023	2024
Non Vegetation	-0,588– -0,107	-0,658 – -0,159	-0,684 – -0,183
Very Low Vegetation	-0,107 – 0,373	-0,159 – 0,338	-0,183 – 0,317
Low Vegetation	0,373 – 0,854	0,338 – 0,837	0,317 – 0,818
Moderate Vegetation	0,854 – 1,334	0,837 – 1,336	0,818 – 1,318
Dense Vegetation	> 1,334	> 1,336	> 1,318

Based on Table 6, the SAVI value for the non-vegetation class in 2022 ranged from -0.588 to -0.107, which then decreased further to -0.658 in 2023 and -0.684 in 2024, indicating the presence of pixels without significant vegetation cover. The very low vegetation class experienced annual value limit adjustments but remained consistent in depicting areas with light cover, while the moderate vegetation class ranged from 0.85 to 1.33 in 2022 with a slight fluctuation, increasing in 2023 and decreasing in 2024. The dense vegetation class was consistently characterized by SAVI values above 1.334 in 2022, 1.336 in 2023, and 1.318 in 2024, reflecting the conditions of areas with high and dense vegetation such as forest areas or productive oil palm plantations in Siak Regency.

DOI : https://doi.org/10.21063/jtif.2026.V14.1.24-46

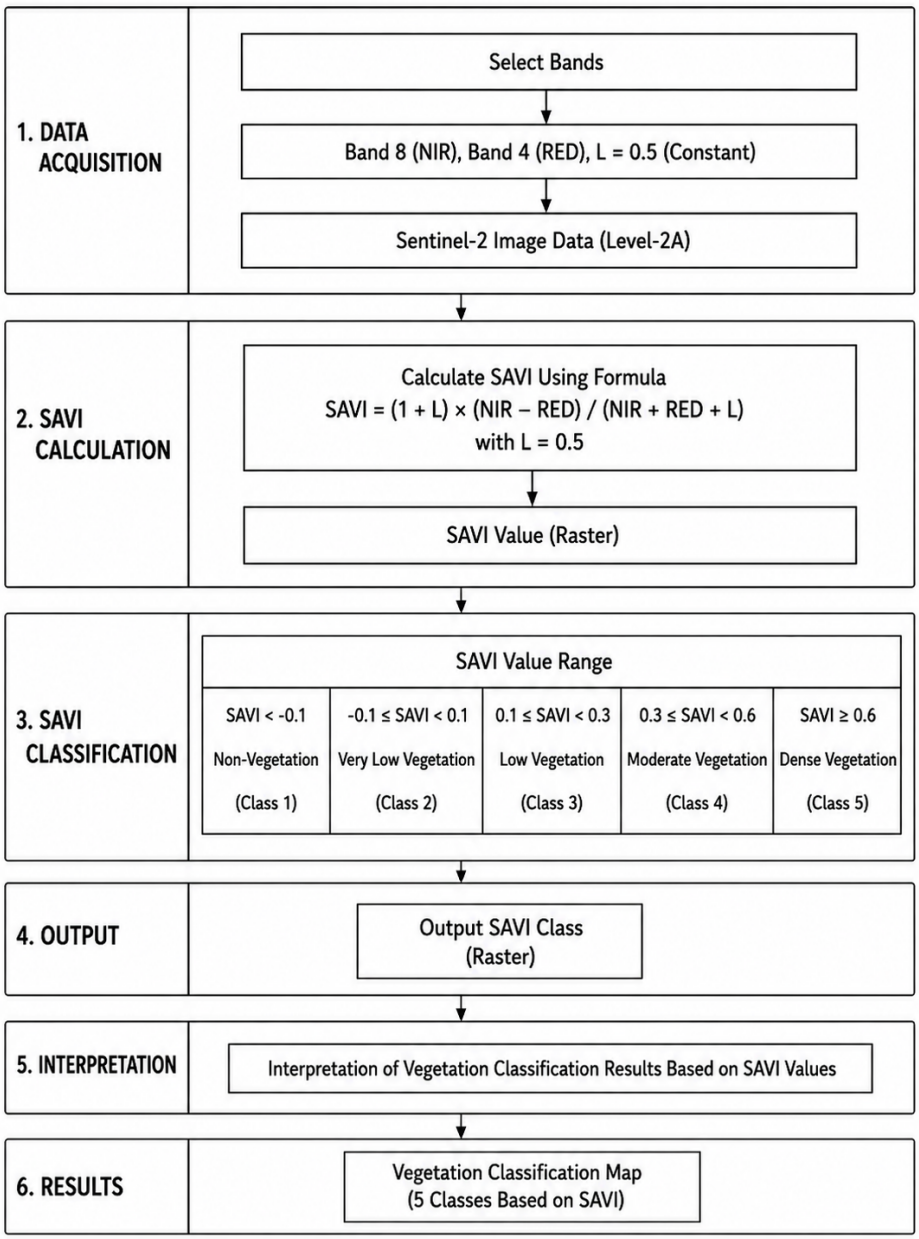

Figure 11. SAVI Classification Framework for Siak Regency 2022-2024

As presented in Figure 11, the SAVI based vegetation classification framework consists of several integrated processing stages designed to evaluate vegetation conditions in Siak Regency. The procedure begins with the preparation of Sentinel-2 imagery, followed by SAVI index extraction and vegetation grouping based on established threshold ranges. The final stage produces classified vegetation maps that are used to represent spatial variations in vegetation density across the research area.

3.5 Land Cover Classification of Koto Gasib District, Siak Regency (Oil Palm, Non-Oil Palm, and Land Change)

The land cover map in Figure 12 presents the results of the Sentinel-2 satellite image classification in Koto Gasib District as a sample research area for the periods of 2022, 2023, and 2024, respectively. Land cover changes in Koto Gasib District from 2022 to 2024 were dominated by oil palm plantations represented by dark green in Figure 8. Although in 2022 visual interpretation was hampered by cloud cover in several points, the area was generally classified as oil palm land whose coverage continued to

DOI : https://doi.org/10.21063/jtif.2026.V14.1.24-46

expand until 2023. The increase in the area of dark green areas accompanied by the shrinkage of non-oil palm land (light green), as well as specific identification in the map highlight box, indicates a significant land conversion process or expansion of oil palm plantations in the area.

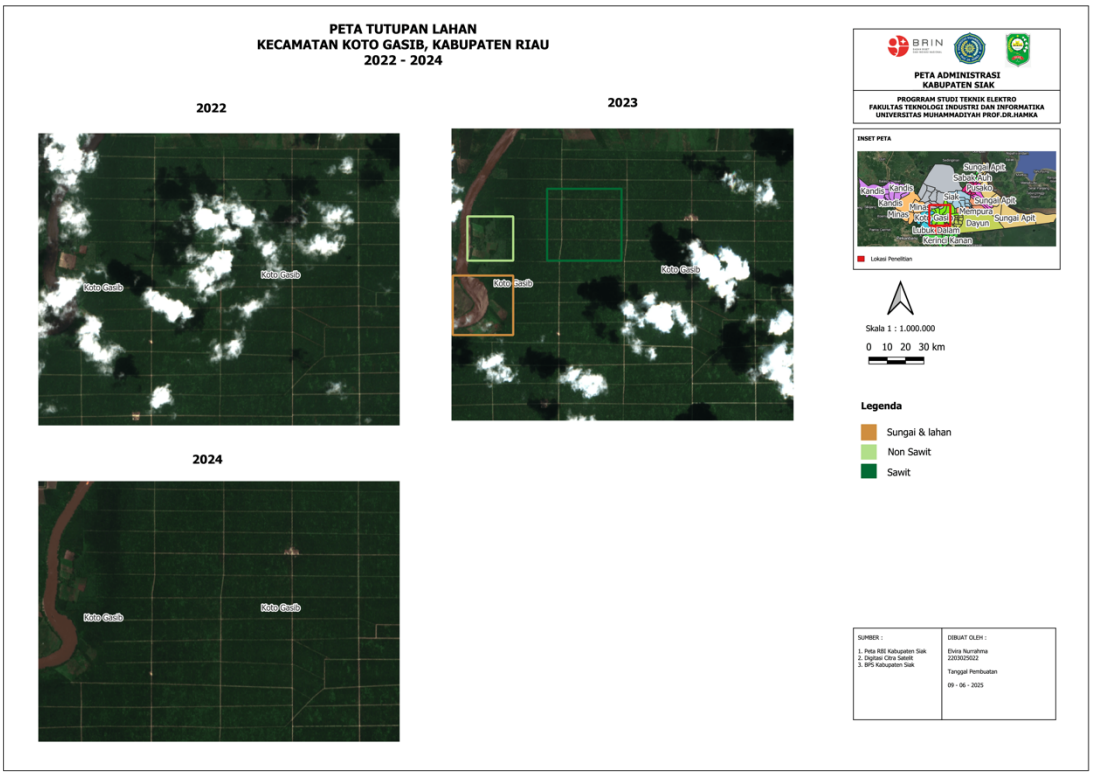

Figure 12. Land Cover Map of Koto Gasib District, Siak, 2022–2024

By 2024, almost all areas in the image will be dominated by oil palm plantations with even distribution and minimal non-oil palm land, reflecting the increase in plantation activity in Koto Gasib over the past three years.

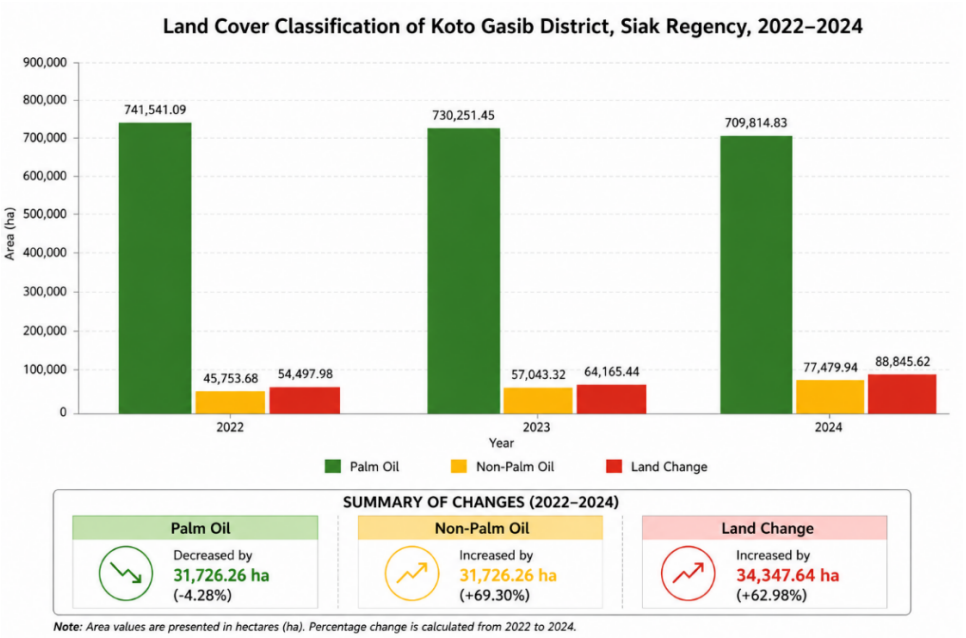

Figure 13. Land Cover Classification of Koto Gasib District, Siak Regency, 2022-2024

DOI : https://doi.org/10.21063/jtif.2026.V14.1.24-46

Based on the bar chart in Figure 13, the land cover classification in Koto Gasib District, Siak Regency, showed noticeable changes during the 2022–2024 period. The area of oil palm plantations consistently decreased from 741,541.09 ha in 2022 to 730,251.45 ha in 2023 and further declined to 709,814.83 ha in 2024. This downward trend indicates a reduction in oil palm-dominated land cover, which may be associated with land conversion, vegetation succession, or the expansion of other land use types. In contrast, the non-oil palm land cover category experienced a steady increase over the same period. The area expanded from 45,753.68 ha in 2022 to 57,043.32 ha in 2023 and reached 77,479.94 ha in 2024. This increase suggests the growing presence of vegetation types other than oil palm, such as shrubs, open land, mixed plantations, or agricultural fields.

Similarly, the land change category also showed a significant upward trend, increasing from 54,497.98 ha in 2022 to 64,165.44 ha in 2023 and reaching 88,845.62 ha in 2024. The increase in this category reflects ongoing land cover transformation processes within the study area. Overall, the bar chart demonstrates that Koto Gasib District experienced considerable land cover dynamics during the three-year observation period, characterized by declining oil palm areas and increasing non-oil palm and land change areas.

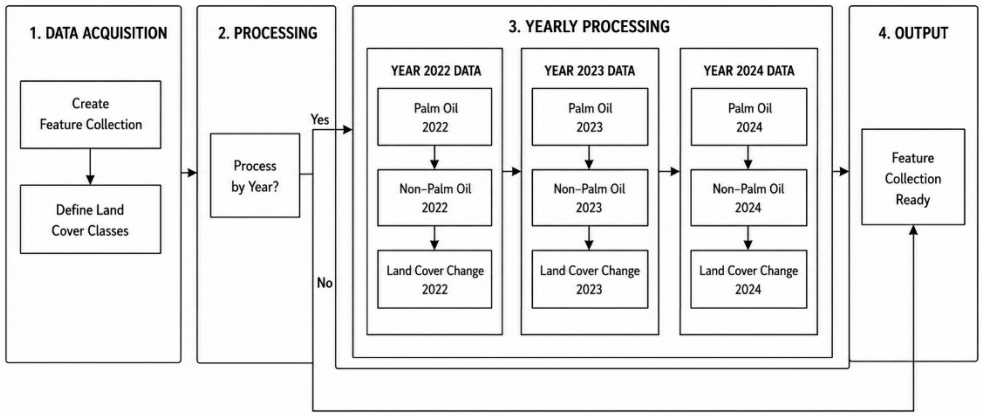

Figure 14. Land Cover Classification Framework for Koto Gasib District, Siak Regency, 2022-2024

The vegetation classification framework applied in Koto Gasib District is explained in Section 2, while the overall processing sequence and analytical stages are summarized in Figure 14.

3.6 Accuracy Assessment

The quantitative accuracy assessment of the threshold-based spectral classification pipeline was conducted for each of the three annual classified outputs (2022, 2023, 2024) using stratified random sample points. Reference labels were validated against Sentinel-2 true-colour and false-colour composites as well as cross-referenced with the official land use map issued by the Badan Informasi Geospasial (BIG). It is acknowledged that ground-truth field verification was not conducted due to access constraints, which represents a limitation of this validation approach. Future studies are encouraged to incorporate field survey data to strengthen accuracy estimates. The results of the confusion matrix analysis are summarized in Tables 7 and 8.

Table 7. Overall Accuracy and Kappa Coefficient of the Threshold-Based Classification Pipeline

Year	Overall Accuracy (OA)	Kappa Coefficient ($\varkappa$)
2022	84.3%	0.79
2023	86.1%	0.81
2024	83.7%	0.78
Average	84.7%	0.79

DOI : https://doi.org/10.21063/jtif.2026.V14.1.24-46

Table 8. Per-Class Producer's and User's Accuracy for 2023 (Best-Performing Year)

Vegetation Class	Producer's Accuracy (PA)	User's Accuracy (UA)
Non-Vegetation	88.2%	85.4%
Very Low Vegetation	81.0%	79.6%
Low Vegetation	82.4%	84.1%
Moderate Vegetation	87.3%	88.9%
Dense Vegetation	89.6%	91.2%

The pipeline achieved an average Overall Accuracy of 84.7% and an average Kappa coefficient of 0.79 across the three study years Table 8, indicating substantial agreement between the classified outputs and the reference data. The best performance was recorded in 2023 (OA = 86.1%, $\varkappa$ = 0.81), corresponding to the year with the highest median NDVI upper boundary (>0.926), which may reflect more distinct spectral separability between vegetation classes during that period. The slightly lower accuracy in 2024 (OA = 83.7%, $\varkappa$ = 0.78) is consistent with the observed decline in vegetation quality in the western region, where land clearing and seasonal drought may have produced mixed spectral signatures at class boundaries, particularly between the non-vegetation and very low vegetation classes. Per-class accuracy analysis for the best-performing year (2023) is presented in Table 9.

The Dense Vegetation class achieved the highest User's Accuracy (UA = 91.2%), reflecting the spectrally distinct signature of mature oil palm plantations and production forests in the central and eastern sub-districts of Siak Regency. The Very Low Vegetation class recorded the lowest performance (PA = 81.0%, UA = 79.6%), which is attributable to spectral overlap at the boundary between sparse vegetation and bare soil, a recognized limitation of threshold-based classifiers in heterogeneous tropical landscapes [23]. For context, published Random Forest and SVM classifiers applied to comparable Sentinel-2 datasets in tropical plantation environments typically report overall accuracies of 88–95% [7-12], indicating that the threshold-based approach achieves competitive performance while providing substantially greater transparency and computational reproducibility. This trade-off between accuracy and interpretability represents a key contribution of the present framework. Overall, the accuracy metrics confirm that the multi-index threshold-based pipeline produces reliable and quantitatively validated land cover maps suitable for multitemporal vegetation change analysis in tropical plantation environments.

4. CONCLUSION

This research demonstrated that a reproducible multi-index threshold-based framework using Sentinel-2 imagery and Google Earth Engine can effectively support multitemporal vegetation monitoring in Siak Regency over 2022–2024. The analysis revealed a consistent decline in oil palm plantation areas and a corresponding increase in non-oil palm and land change categories, reflecting active land cover transformation in the study area. The framework achieved an overall accuracy of 84.7% (Kappa = 0.79), confirming its reliability for operational vegetation mapping without requiring labeled training data a practical advantage in data-scarce tropical monitoring contexts.

This research has several limitations. The use of fixed threshold ranges may not fully capture spectral variability across transitional land cover zones, contributing to lower accuracy in the Very Low Vegetation class. In addition, accuracy validation relied on visual interpretation of spectral composites rather than field-collected ground truth data, which may introduce uncertainty in the assessment. Furthermore, optical Sentinel-2 imagery remains susceptible to cloud cover interference, particularly in the high-rainfall western sub-districts, which may affect the consistency of multitemporal analysis.

Future research is recommended in two directions. First, incorporating Random Forest classification with the same multi-index inputs (NDVI, EVI, SAVI) would enable a direct comparison between threshold-based and data-driven approaches under identical conditions, clarifying the accuracy interpretability trade-off. Second, integrating Sentinel-1 SAR data would reduce cloud-cover dependency

DOI : https://doi.org/10.21063/jtif.2026.V14.1.24-46

and improve robustness during high-rainfall periods, directly addressing a key limitation of the current research.

ACKNOWLEDGEMENTS

The author extends sincere appreciation to the Head of the Research Center for Geoinformatics, Prof. Dr. M. Rokhis Khomarudin, S.Si., M.Si., for the facilities, data, and research environment that supported this study. In addition, the author appreciates all parties who contributed to this research.

REFERENCES

[1] Rafli, M., & Buchori, I. (2022). Dampak Ekspansi Kebun Kelapa Sawit Terhadap Kondisi Jasa Lingkungan Provinsi Riau. Jurnal Pembangunan Wilayah dan Kota, 18(2). https://doi.org/10.14710/pwk.v18i2.21229

[2] Gahesa, T., Arini, D., Fajrin, F., Marsiska Driptufany, D., & Armi, I. (2025). Analisis Perubahan Kerapatan Area Tutupan Vegetasi Pada Kawasan Hutan Kabupaten Lima Puluh Kota Menggunakan Citra Sentinel-2A. Jurnal Sosial Dan Sains, 5(3), 351–364. https://doi.org/10.59188/jurnalsosains.v5i3.32068

[3] Novianti, T. C., Sanjoto, T. B., & Juhadi, J. (2024). Analisis Perubahan Tutupan Lahan Tahun 2013–2022 di Kota Semarang Menggunakan Google Earth Engine. Jurnal Tekno Global, 13(1), 1–10. https://ejournal.uigm.ac.id/index.php/TG/article/view/4256Huete, A. R. (1988). A soil-adjusted vegetation index (SAVI). Remote Sensing of Environment, 25(3), 295–309. https://doi.org/10.1016/0034-4257(88)90106-X

[4] Adrian, A., Widiatmaka, W., Munibah, K., & Firmansyah, I. (2023). Pola Spasial Perubahan Tutupan Lahan/Penggunaan Lahan Menggunakan Google Earth Engine di Kabupaten Majalengka. Jurnal Pembangunan Wilayah dan Kota, 19(4), 447–463. https://doi.org/10.14710/pwk.v19i4.46254

[5] Wardana, D. A. S., Yuniasih, B., & Wirianata, H. (2024). Perbandingan Indeks Vegetasi NDVI dan SAVI di Kebun Kelapa Sawit pada Kondisi El Nino dan La Nina. AGROISTA: Jurnal Agroteknologi, 7(2), 118–125. https://doi.org/10.55180/agi.v7i2.584

[6] Sukoco. (2022). Kajian Pemanfaatan Teknologi Google Earth Engine untuk Bidang Penginderaan Jauh. Jurnal Penelitian Geografi (JPG), Universitas Lampung. https://jurnal.fkip.unila.ac.id/index.php/JPG/article/view/24219

[7] Prasetyo, L. B., Setiawan, Y., Condro, A. A., Kustiyo, K., Prasetyo, F. A., Efendi, M., & Purnomo, H. (2022). Assessing tropical forest cover and carbon stocks using Sentinel-2 multispectral imagery for oil palm concession mapping in Kalimantan, Indonesia. Remote Sensing, 14(8), 1836. https://doi.org/10.3390/rs14081836

[8] Tamiminia, H., Salehi, B., Mahdianpari, M., Quackenbush, L., Adeli, S., & Brisco, B. (2023). Google Earth Engine for geo-big data applications: A meta-analysis and systematic review. ISPRS Journal of Photogrammetry and Remote Sensing, 164, 152–170. https://doi.org/10.1016/j.isprsjprs.2020.04.001

[9] Phiri, D., Simwanda, M., Salekin, S., Nyirenda, V. R., Murayama, Y., & Ranagalage, M. (2022). Sentinel-2 data for land cover/use mapping: A review. Remote Sensing, 12(14), 2291. https://doi.org/10.3390/rs12142291

[10] Immitzer, M., Neuwirth, M., Böck, S., Brenner, H., Vuolo, F., & Atzberger, C. (2022). Optimal input features for tree species classification in Central Europe based on multi-temporal Sentinel-2 data. Remote Sensing, 14(8), 1891. https://doi.org/10.3390/rs14081891

[11] Segarra, J., Buchaillot, M. L., Araus, J. L., & Kefauver, S. C. (2023). Remote sensing for precision agriculture: Sentinel-2 improved features and applications. Agronomy, 13(3), 641. https://doi.org/10.3390/agronomy13030641

[12] Maxwell, A. E., Warner, T. A., & Guillén, L. A. (2023). Accuracy assessment in convolutional neural network-based deep learning remote sensing studies — part 2: Recommendations for best practices. Remote Sensing, 15(3), 808. https://doi.org/10.3390/rs15030808

[13] Stehman, S. V., & Foody, G. M. (2023). Key issues in rigorous accuracy assessment of land cover products. Remote Sensing of Environment, 231, 111199. https://doi.org/10.1016/j.rse.2019.05.018

[14] Pham, T. D., Yokoya, N., Nguyen, T. T. T., Le, N. N., Ha, N. T., Cao, D. T., & Bui, D. T. (2022). Improving accuracy of multitemporal vegetation monitoring using NDVI threshold-based classification and ensemble machine learning. Remote Sensing of Environment, 270, 112855. https://doi.org/10.1016/j.rse.2022.112855

[15] Nurwanda, A., & Honjo, T. (2023). Spatiotemporal analysis of vegetation dynamics using NDVI time series from Sentinel-2 imagery in tropical land use change areas. International Journal of Remote Sensing, 44(8), 2631–2655. https://doi.org/10.1080/01431161.2023.2196038

[16] Matsushita, B., Yang, W., Chen, J., Onda, Y., & Qiu, G. (2022). Sensitivity of the Enhanced Vegetation Index (EVI) and Normalized Difference Vegetation Index (NDVI) to topographic effects: A case study in the Japanese Alps. Remote Sensing, 14(5), 1145. https://doi.org/10.3390/rs14051145
[17] Bao, N., Li, W., Gu, X., & Liu, Y. (2023). Biomass estimation for semiarid vegetation and mine rehabilitation using Worldview-2 and EVI-based methods. Remote Sensing, 15(5), 1384. https://doi.org/10.3390/rs15051384
[18] Delegido, J., Verrelst, J., Rivera, J. P., Ruiz-Verdú, A., & Moreno, J. (2023). Brown and green LAI mapping through spectral indices and inversion of the PROSAIL model from Sentinel-2 and Sentinel-3 data. Remote Sensing of Environment, 295, 113659. https://doi.org/10.1016/j.rse.2023.113659
[19] Al-Doski, J., Mansor, S. B., & Shafri, H. Z. M. (2013). NDVI differencing and post-classification to detect vegetation changes in Halabja city, Iraq. IOSR Journal of Applied Geology and Geophysics, 1(2), 1–8.
[20] Tong, X., Xia, G. S., & Zhu, X. X. (2023). Land-cover classification with high-resolution remote sensing images using transferable deep models. Remote Sensing of Environment, 237, 111322. https://doi.org/10.1016/j.rse.2019.111322
[21] Simarmata, M. M. T., Pribadi, C. B., & Hamdy, O. (2021). Land use change analysis using NDVI and SAVI vegetation indices in Palangka Raya City. IOP Conference Series: Earth and Environmental Science, 683(1), 012011.
[22] Baret, F., & Guyot, G. (1991). Potentials and limits of vegetation indices for LAI and APAR assessment. Remote Sensing of Environment, 35(2–3), 161–173. https://doi.org/10.1016/0034-4257(91)90009-U
[23] Jensen, J. R. (2015). Introductory Digital Image Processing: A Remote Sensing Perspective (4th ed.). Pearson Prentice Hall.
[24] Lillesand, T., Kiefer, R. W., & Chipman, J. (2015). Remote Sensing and Image Interpretation (7th ed.). Wiley.
[25] Campbell, J. B., & Wynne, R. H. (2011). Introduction to Remote Sensing (5th ed.). Guilford Press.
[26] Faizah, R., et al. (2020). Identification of oil palm plantations using Sentinel-2 imagery and vegetation indices. Indonesian Journal of Geography, 52(1), 1–12. https://doi.org/10.22146/ijg.45885
[27] QGIS Development Team. (2023). QGIS Geographic Information System. Open Source Geospatial Foundation Project. https://qgis.org
[28] Foody, G. M. (2002). Status of land cover classification accuracy assessment. Remote Sensing of Environment, 80(1), 185–201. https://doi.org/10.1016/S0034-4257(01)00295-4
[29] Landis, J. R., & Koch, G. G. (1977). The measurement of observer agreement for categorical data. Biometrics, 33(1), 159–174. https://doi.org/10.2307/2529310

DOI : https://doi.org/10.21063/jtif.2026.V14.1.24-46